Dhaka Univ. J. Sci. 74(1): 111-121, 2026 (January)
Prof. M. Muhibur Rahman Memorial Issue
ISSN 1022 - 2502, E-ISSN 2408- 8528
DOI: https://doi.org/10.3329/dujs.v74i1.80460

Optical Band Gap Tailoring and Enhanced Electrical Performance of Cu-Doped ZnO Thin Films via Sol-Gel Fabrication

Kazi Zahanara Islam[1], Muhammad G. Azam,[1,2] and Md. Borhanul Asfia[3]

[1]*Department of Physics, Bangladesh University of Engineering and Technology, Dhaka-1000, Bangladesh.*
[2]*Bangladesh Atomic Energy Regulatory Authority, 12/A Shahid Shahabuddin Rd, Dhaka-1207, Bangladesh and*
[3]*Department of Physics, Jashore University of Science and Technology, Jessore, Bangladesh*

(Received : 11 March 2025 ; Accepted : 29 December 2025)

Abstract

Copper-doped zinc oxide (CZO) thin films have been widely investigated owing to their potential application in optoelectronic devices. In this study, we report the optical and electrical properties of zinc oxide (ZO) and copper-doped zinc oxide (CZO) thin films prepared using the sol-gel method. The copper concentration was changed to investigate the impact of copper doping on the optical and electrical properties of the films. The absorption spectra revealed that copper doping caused the absorption edge to shift to the red, which triggered an increase in bandgap energy of ZO from 3.16 eV to 3.47 eV. Electrical measurements were used to calculate the electrical resistivity of the thin films. For ZO and CZO, copper doping resulted in a decrease in resistivity from 2.272-cm to 0.904-cm and an increase in carrier concentration. This property can be useful in some conditions, where low resistivity and high conductivity are required, such as transparent conductive coatings for optoelectronic devices. The optical analysis shows how the Urbach energy of the film increases with the rise in Cu doping percentage.

Keywords: Thin Films, copper-doped zinc oxide, Dip-coating, Optical property, Electrical property, Band gap, Urbach energy.

I. Introduction

Research on nanocrystalline ZO thin films has been undergoing significant development because of their wide range of applications in optics, electronics, photonics, etc. ZO is an n-type II-IV group multifunctional semiconductor material with a wide direct ≈ 3.3 eV optical band gap at room temperature and with a free binding energy of 60 meV[1,2]. Moreover, it is one of the noteworthy transparent conducting oxides (TCO) with a hexagonal wurtzite structure associated with unintentional n-type conductivity due to the existence of free charge carriers created from[3] point defects. These point defects arise from oxygen vacancies and Zn interstitials[4]. In the fabrication of optoelectronic devices, ZO has faced a serious limitation because its electrical conductivity depends on native point defects. However, it has good transparency and room temperature luminescence, which has made it a promising material for a plethora of applications[5]. Many research groups have been working vigorously to regulate the n-type conductivity and obtain improved optical and electrical properties of ZO by using an apposite substitutional compound of ZO. In this regard, transition metals (TMs) are the appropriate candidate as a dopant. TM ions give rise to unpaired electrons by filling *d* and *f* shells correspondingly[6], and consequently, new energy levels appear inside the band gap. Thus, it is rational to predict that the accumulation of such dopants may enhance the electrical conductivity as well as affect the optical properties of ZO. In recent years, many researchers have been analyzing the doping effect of TMs, for instance Ni (nickel)[7], Co (cobalt)[8], manganese (Mn)[9], copper (Cu)[10], as well as alkaline earth metals such as magnesium (Mg)[11], etc. Kyoung-Tae et al.[7] found that the optical and electrical properties of Ni-doped ZnO thin films were strongly affected by doping concentration. Georgeta et al.[8] showed that deposited films of different Co doping concentrations were nanostructured, having a thickness of less than 1 μm. Dan et al.[9] found that pure and Mn-doped ZO exhibit room temperature photoluminescence. On the other hand, Agarwal et al.[11] reported that pure and Cu doped ZO thin films demonstrated unique room temperature ferromagnetism along with green photoluminescence. Among these, TM Cu is the most promising of all because of the comparable ionic radii of Zn^{2+} (0.74 Å) to that of Cu^{2+} (0.73 Å)[12]. So, Cu has the feasibility to form a unique compound by incorporating into the ZO matrix. Moreover, very few studies have been done on Cu doped ZO thin films by the sol-gel method so far. Most of the works published on Cu doped ZO are based on the nanoparticle synthesis process[13,14]. A detailed optical and electrical study on pure and Cu doped ZO is still very few. ZO thin films are already established as a potential transparent conducting oxide and by using an ambient dopant, its properties can be tailored for optoelectronic applications. In this study, ZO and CZO thin films were deposited by the sol-gel dip coating technique. The deposition technique has a key impact on controlling the structural, surface morphological, optical, and electrical properties of the films. Several techniques have been used to deposit ZO thin films, for instance, chemical bath deposition, sol-gel dip coating, sputtering, spray pyrolysis, drop-casting[10], etc. Among these processes, sol-gel dip coating is adaptable, economical, and dominant along with large area deposition. Sol-gel dip coating exhibits excellent compositional control, better homogeneity, and lower crystallization temperature[10]. These advantages have inspired us to choose the sol-gel

*Author for correspondence. e-mail: islam.zahanara@gmail.com

dip-coating technique for the fabrication of ZO and CZO thin films and to analyze their optical and electrical properties.

II. Materials and Methods

Fabrication of ZnO and ZnO: Cu Thin Films

Zinc acetate dihydrate [$Zn(CH_3COO)_2.2H_2O$] and copper acetate [$Cu(CH_3COO)_2$] have been used as precursor materials for Zn and Cu, respectively, to synthesize ZO and CZO thin films by using the sol-gel dip-coating technique. Ethanol and Di-ethanol amine (DEA) have been used as solvents and stabilizers, respectively. A certain amount of precursor solution was prepared by dissolving [$Zn(CH_3COO)_2.2H_2O$] in ethanol and kept stirring for 2 h. Then stabilizer and deionized water were added to the precursor solution, and the mixture was stirred for another 2 h at room temperature to obtain a homogeneous solution. Ultrasonically cleaned microscopic glass substrates (10 mm × 15 mm × 1.5 mm) were dipped into the homogenous precursor solution to deposit thin films. The deposition rate was kept constant at 10 mm/min. The fabricated films were dried at room temperature and calcinated at 350 °C to remove organic elements. To synthesize CZO thin films, an appropriate amount of [$Zn(CH_3COO)_2.2H_2O$] and Cu source was dissolved into ethanol to make precursor solutions of different concentrations (4 and 8 wt.%). The thickness of the films has been calculated by the Fizeau fringes at reflection method. The whole thin film deposition procedure has been shown through the following flow chart in Fig. 1.

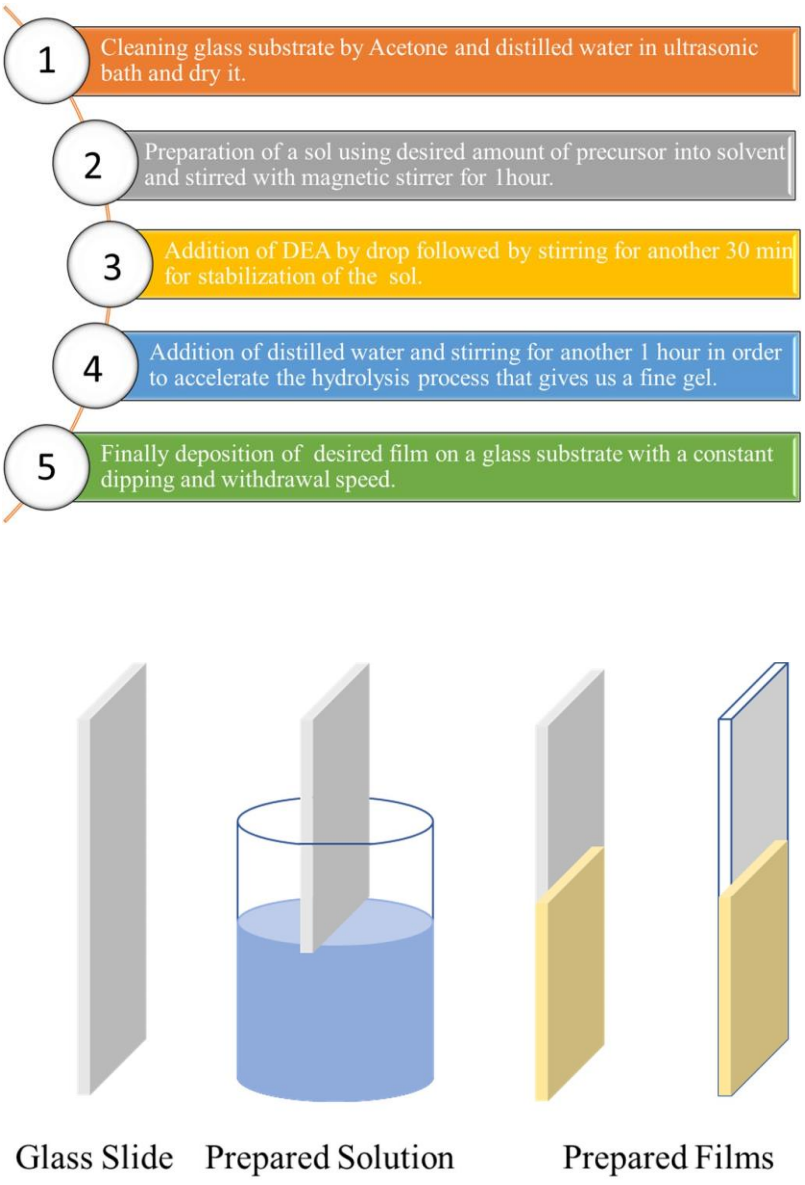

Fig. 1. Schematic diagram of sol-gel dip coating procedure.

Fig. 1 displays a schematic presentation of the sol-gel dip coating method, whereas Fig. 2 depicts the optical clarity of the coated films. The films were placed above printed alphabets to clarify the transparency of the ZO and CZO thin films at the time of taking photos.

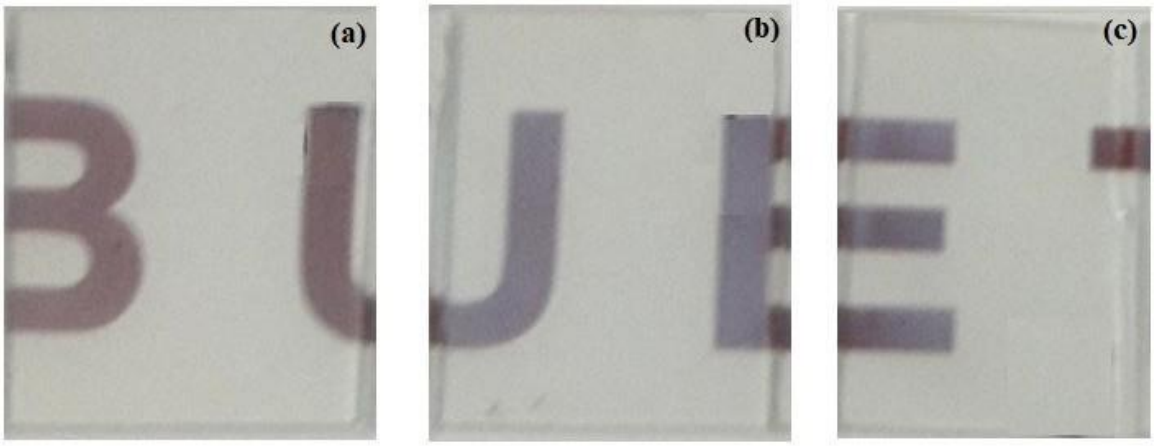

Fig. 2. ZO and CZO thin films (a) ZO (b) 4 wt.% CZO (c) 8 wt.% CZO calcinated at 350^{O} C.

Optical and Electrical measurements

By using the absorbance and transmittance of the deposited films, the absorption coefficient (α), refractive index (n), extinction coefficient (k), and the optical band gap energy (E_g) have been calculated. The data were taken within the spectral wavelength 200 nm to 1100 nm from a UV-visible spectrometer (Dynamica HALO DB-20S). Optical measurements were conducted at room temperature. A four-point probe method has been used to measure the sheet resistance of ZO and CZO thin films.

III. Results and Discussion

Optical Properties Studies

The optical nature of semiconductor thin films vigorously depends on the deposition technique, deposition condition, surface structure, and the effect of the circumstance on the deposited materials. Consequently, we need to study the optical nature of the synthesized thin films to analyze their reliability for fabricating a particular device. The phenomenon of increasing transmittance, as shown in **Fig. 3 (A)**, with growing Cu doping in ZO thin films, despite an increase in the optical bandgap, can be attributed to several underlying mechanisms.

Copper doping introduces additional energy levels within the ZO bandgap, leading to the formation of impurity or defect states. These impurity states act as trapping centers for electrons, reducing the recombination rate of electron-hole pairs generated by incident photons. As a result, a larger number of electrons are available for conduction, leading to enhanced electrical conductivity and increased transmittance. The introduction of copper dopants modifies the electronic band structure of the ZO thin film. The impurity states created by copper doping can induce strain and alter the energy levels within the material. This modification can result in a shift of the energy levels, including the valence band and conduction band edges. Consequently, the optical bandgap, which represents the energy difference between these two bands, increases as shown later in **Fig. 3 (D)**.

The increase in the optical bandgap implies that higher energy photons, corresponding to shorter wavelengths, are absorbed to a lesser extent by the material. As a result, a larger portion of the incident light in the visible spectrum is transmitted through the CZO thin film, leading to increased transmittance. Moreover, copper doping can also influence the defect density and crystal quality of the ZO thin film. The incorporation of copper ions can reduce the concentration of defects and impurities, which act as scattering centers for light. This reduction in defect density contributes to improved light transmission and increased transmittance[54].

It is important to note that the relationship between Cu doping concentration, optical bandgap, and transmittance is not linear. Beyond a certain threshold, excessive copper doping can introduce additional scattering centers or impurity states, which can lead to decreased transmittance due to increased light absorption or scattering.

The increase in transmittance with increasing Cu doping percentage in ZO thin films, despite an increase in the optical bandgap, can be attributed to the increased availability of free electrons for conduction, strain-induced modifications in the band structure, and reduced defect density. These factors collectively contribute to the enhanced transmittance of the CZO thin films in the visible spectrum.

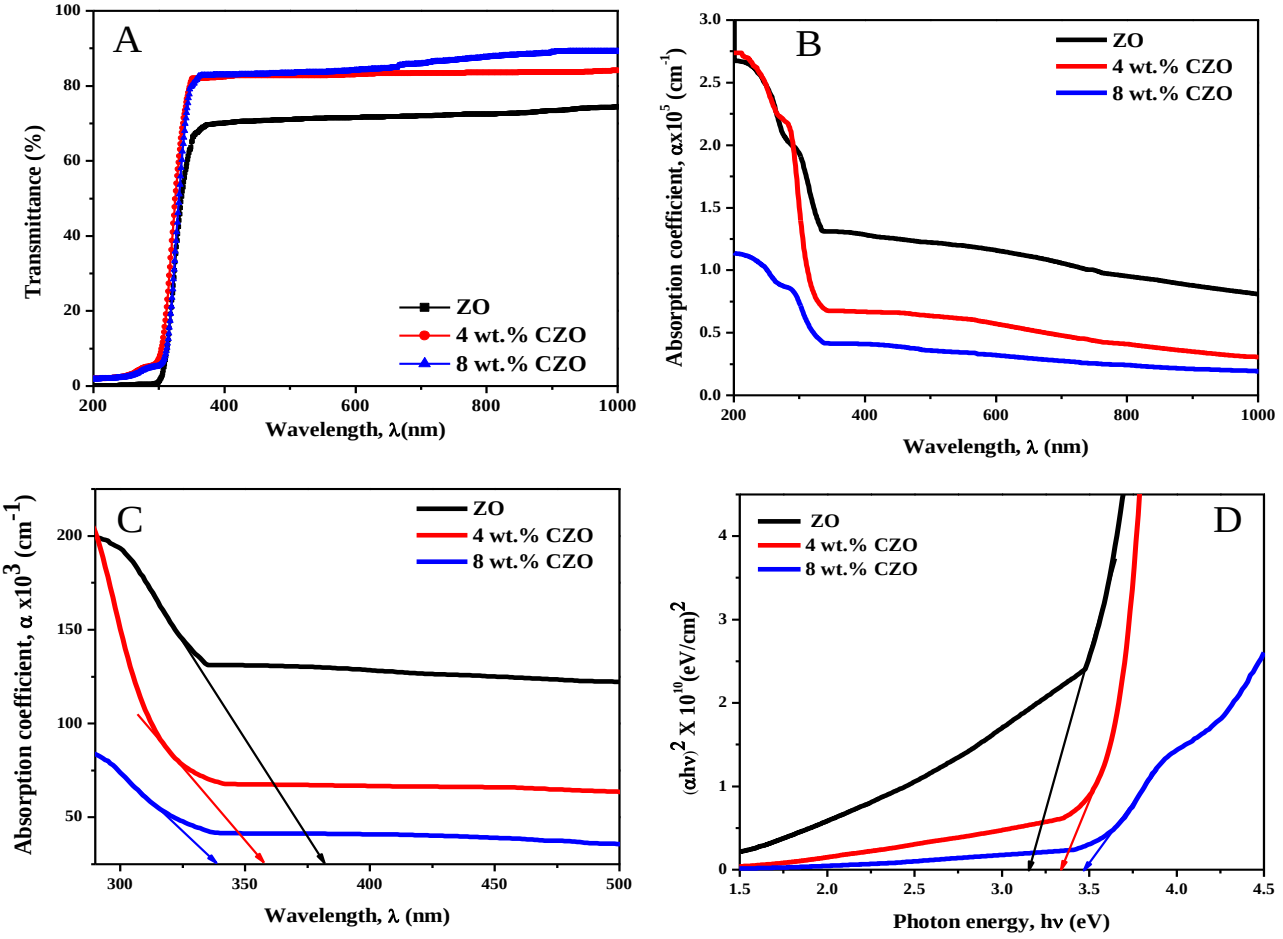

Fig. 3. (A) Transmittance spectra for ZO and CZO thin films, (B) Absorption coefficient spectra for ZO and CZO thin films, (C) Absorption edge spectra for ZO and CZO thin films, and (D) Direct bandgap spectra for ZO and CZO thin films.

The electronic state of any semiconductor at higher energy can be determined by studying the absorption coefficient curve structure of that material. In contrast, the lower energy part gives us information about the atomic vibration[15,16]. Moreover, ZO is one of the well-received transparent conducting oxides. Apparently, CZO becomes optically responsive, which makes the optical measurement more crucial. The absorption coefficient (α) of thin films can be calculated from the absorbance (A), by using the following formula[17]:

$$\alpha = \frac{2.303A}{t} \quad (1)$$

Where t is the thickness of the film. The wavelength versus absorption coefficient spectra for ZO and CZO for different percentages have been shown in **Fig. 3 (B)**. The sequence of the curves from 0 wt.%, 4 wt.%, and 8 wt.% doping concentration is discontinuous in nature. This may have happened because of the irregular nature of the thickness of the deposited films. After doping film thickness seems to increase. This increase in film thickness can be described by the mass action law, which states that the rate of deposition is determined by the added dopant[18]. When the dopant concentration is too high, the oxygen from H_2O needed to foster the deposition rate is inadequate. Consequently, different doping concentrations result in different growth rates corresponding to varying film thickness[19].

Absorption coefficient of thin films influenced by the doping percentage as well, and in this work, 4 wt % CZO exhibits the highest value of the α. Furthermore, the α declines with the increase in Cu percentage. This trend may be attributed to the absorbing nature of Cu atoms. However, the α of all the samples has a higher (10^5 cm^{-1}) order value. The absorption edge has been calculated for each composition by extending a line from the baked portion of the absorption coefficient spectra, which intercepts the photon wavelength axis at a certain point. The intersection point has given the absorption band edge value for each sample. The impact of doping concentration on the absorption edge is shown in **Fig. 3 (C),** and the corresponding values are tabulated in Table 1. The absorption edge value shifted towards lower wavelength with the increase of Cu wt % within the visible wavelength region. However, the photon energy (hν) changes

increasingly from 3.208 eV (λ ≈ 390 nm) to 3.616 eV (λ ≈ 346 nm) for ZO and different percentages of CZO. This shifting nature is desired as it contributes to the change in band gap energy for which transitional metals are doped into semiconductors[20]. This result is in compliance with the result calculated by Joshi et al.[21].

Optical density (D_{opt}) of thin films depends upon its thickness and the absorbing nature of the synthesized materials. The optical density of ZO and CZO at different concentrations has been calculated by using the equation: $D_{opt}=\alpha t$, where **t** is the thickness of the films[22,23]. Since the absorption coefficient α depends on thickness, D_{opt} spectra showed quite a similar nature whether plotted against the wavelength of incident light or photon energy (hν). **Fig. 4** shows the photon energy versus optical density graph.

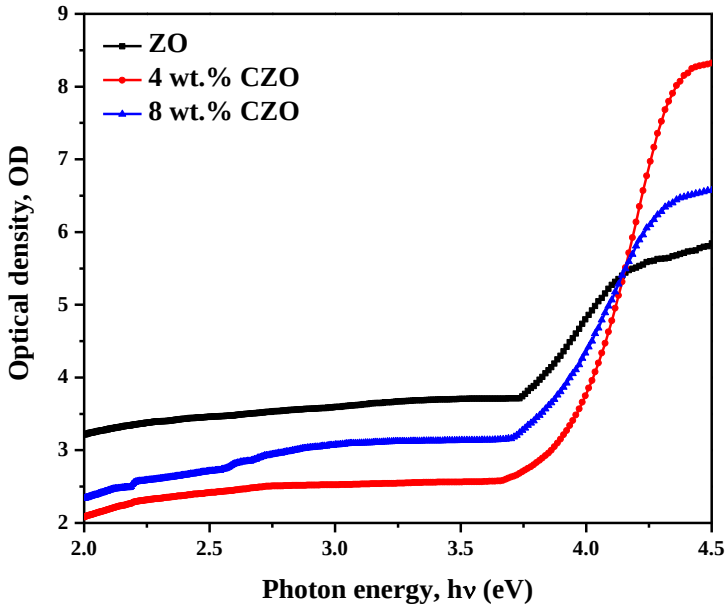

Fig. 4. Optical density spectra for ZO and CZO

On the other hand, absorption coefficient (α) and band gap energy are closely related by the following equations (2) and (3),

$$\alpha = \frac{\beta}{h\vartheta}(h\vartheta - E_g)^n \quad (2)$$

$$(\alpha h\vartheta)^{\frac{1}{n}} = \beta(h\vartheta - E_g) \quad (3)$$

Here β is a constant which is known as the band tailing parameter and n is the transition mode power factor. All those factors depend on the structural property of the synthesized films, whether they form a crystalline composition or not. If it is a crystalline film, then it has a direct transition, and for a non-crystalline film indirect transition has occurred according to the Tauc formula [24,25]. **Fig. 3 (D)** shows the direct optical band gap determination graph for all the samples. By extending the tangent line from the linear portion of the curve to intercept the x-axis at y = 0, we can calculate the value of the optical energy gap. **Table 1** shows the estimated band gap values. The E_g increased with the increase of Cu doping concentration from 3.16 eV to 3.47 eV. Joshi. et al.[21] reported an increase in band gap energy for CZO. Samavati Alireza et al. [26] have recorded a consecutive increment in band gap value with the addition of Cu. The band gap value increased from 3.25 to 3.35 for pure ZO and 0.05 CZO thin films deposited by the sol-gel method. Arindam et al.[27] have reported a band gap widening of 3.42, 3.50, and 3.54 eV for undoped, 1 wt.% CZO and 3 wt.% CZO nanoparticles. Amanullah et al.[28] have observed a little increase in the optical band gap of 3.248 eV for 8 wt.% CZO from 3.239 eV for pure ZO synthesized by the sol-gel method. Labhane et al.[29] have worked for Cu doped ZO nanoparticles and have calculated an increase in band gap energy after 0.03% of CZO. The value of E_g is 3.46 eV and 3.55 eV for ZO and 0.03 % CZO, respectively and mainly referred Burstein-Moss effect for band gap widening.

The changes in optical band gap energy in semiconductor materials depend on deposition procedure, chemical composition, the arising of defects, crystal size, as well as due to the increase in carrier concentration known as the Burstein-Moss (BM) effect[30-32]. The excess electron levels of a heavily doped semiconductor stayed close to the conduction band minimum. Moreover, Pauli's Exclusion principle suppresses states to be singly occupied due to the vertical optical transition of ZO, which leads to the need for additional energy to excite valence electrons to the higher states within the conduction band[33]. Furthermore, Cu doping introduces additional energy levels within the ZO

bandgap[34]. These localized energy levels, arising from the presence of Cu atoms and their interactions with the surrounding ZO lattice, can act as trap states for electrons. The introduction of these trap states effectively increases the energy required for electrons to transition from the valence band to the conduction band, resulting in an increased optical bandgap[35]. Again, at higher Cu doping concentrations, nanocrystalline regions may form within the ZO thin film[36]. These nanocrystals can exhibit quantum confinement effects, where the size of the nanocrystal becomes comparable to the wavelength of the electron wavefunction. In this confined state, the energy levels become quantized, resulting in a modification of the band structure. The confinement-induced changes can lead to an increase in the bandgap energy, thereby affecting the optical properties of the material.

Table 1. The value of the band edge, direct optical band gap, refractive index, and Urbach energy of the chalcogenide thin films of ZO and CZO

Composition	Wavelconth (nm)	Band Edge, (eV)	Optical Band Gap, E_g (eV)	Refractive Index, n	Urbach Energy, E_u (eV)
ZO	391.52	3.199	3.16	2.341	0.19
4% CZO	346.64	3.616	3.34	2.309	0.22
8% CZO	351.49	3.565	3.47	2.287	0.75

Thin films have exhibited some unique properties due to their surface attribute. ZO and CZO thin films have a high optical absorption coefficient, so it can be said that most of the incident light energy that enters the deposited thin film surface is absorbed, and only a small portion of that energy is reflected from the surface. There are several parameters related to energy absorption, for instance, composition, doping percentage, thickness, conductivity, and extinction coefficient value of the deposited films. Therefore, absorption of energy within the surface of a thin film is closely related to skin effect or skin depth and optical conductivity. In the earlier part of the discussion, optical conductivity has been described. Now, the impacts of skin depth or penetration depth have been analyzed. Skin depth depends on photon current density, whose value is decreased exponentially from the film surface to the middle due to some intrinsic effects, i.e., density of films, surface morphology, and microstructure of the deposited films[37]. Skin depth is defined as the corresponding thickness at which the photon current density turns into 1/e of the value at the surface. Moreover, penetration depth is correlated with the optical attributes of the films since the optical band gap vigorously controls the conductivity of any semiconductor material[22]. Equation (4) of skin depth (δ) is expressed by a simple relation with the α,

$$\delta = \frac{1}{\alpha} \tag{4}$$

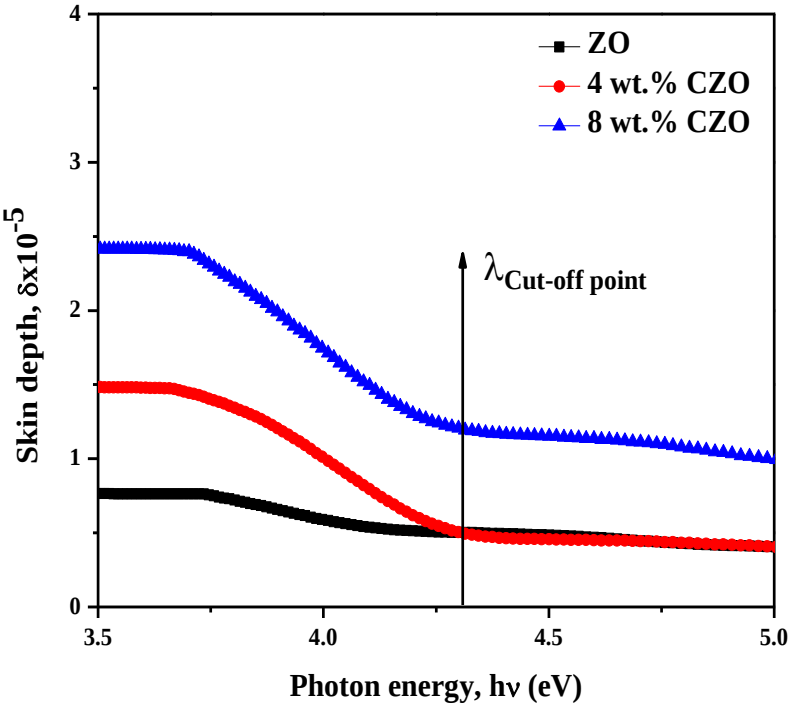

Fig. 5. Skin depth vs photon energy spectra for ZO and CZO thin films.

Here, the skin depth of ZO and CZO films was calculated using the above equation and represented in **Fig. 5.** The graph is plotted with respect to the incident energy and shows that the skin depth of the deposited films increased with the increase of Cu doping percentage, but at lower photon energy. As the photon energy increases δ decreases gradually for all the samples, and after a certain point, the lines become quite linear.

That particular point is called the cut-off point, and the corresponding wavelength (λ) is called the cut-off wavelength. In this case, the $E_{cut\text{-}off\ point}$ hν = 4.31 eV and $\lambda_{cut\text{-}off}$ = 464 nm. After crossing the cut-off point, the absorption of photon energy disappears, and the amplitude dips due to passing a long distance within the film thickness. Therefore, δ becomes transmittance dependent[38]. Similar results were obtained by Radaf et al.[39].

Refractive index and extinction coefficient are addressed as the "fingerprint of material". The refractive index is a fundamental optical property that describes how light propagates through a material. It quantifies the ratio of the speed of light in a vacuum to the speed of light in the material. The refractive index determines how light is bent or refracted when it passes from one medium to another. So, it's crucial to analyze those properties for ZO and CZO films. The optical constant refractive index can be determined from the corrected transmittance T (λ) and reflectance R (λ) using a developed computational method.[40, 41]

$$T(\lambda) = \frac{4n}{(n+1)^2} \quad \text{and} \quad R(\lambda) = \frac{(n-1)^2}{(n+1)^2} \tag{5}$$

Where n is the refractive index of thin films. Films having a high absorption coefficient similar to our current report, the R at the vacuum-film interface has to take into account the value of the k so that R(λ) can be rewritten as (Kramers-Kronig relation) [42]

$$R(\lambda) = \frac{[(n-1)^2 + k^2]}{[(n+1)^2 + k^2]} \tag{6}$$

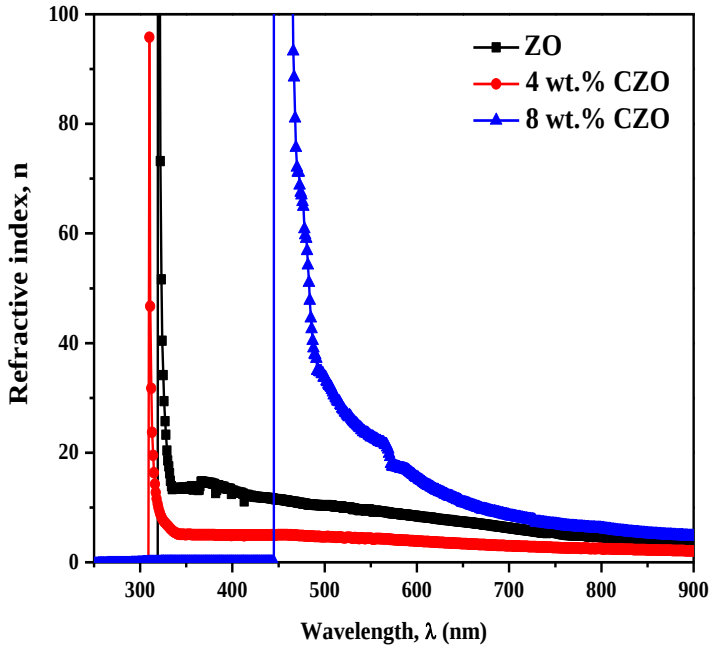

Fig. 6. Refractive Index vs wavelength spectra for ZO and CZO thin films.

Fig. 6 illustrates the refractive index vs wavelength curve, which indicates discontinuous trade. The refractive index value decreased with Cu doping; however, further doping causes an increase in the value, and the transition point shifts from 330 nm to 526 nm. After the transition, the curves become linear. The calculated value of n is tabulated in Table 1 and calculated by using the Moss equation.[43, 44]

$$n^4 = \frac{K}{E_g}, Where\ K = 94\ eV \tag{7}$$

The refractive index primarily depends on the polarization of ions within a material. When light passes through a material, it polarizes the ions of the material; in turn, the propagation speed of the light wave is affected. The propagation speed reduced as polarization of ions increases by absorbing light energy; consequently, refractive index increases[45]. At the lower wavelength region (300 nm ≤ λ ≤ to 400 nm), ZO and CZO exhibit a high refractive index, which means the ions of the deposited materials are strongly polarized within this wavelength region. This high refractive index also indicates the equivalence of plasma

frequency and the frequency of the incident photon. But at longer wavelength (550 nm ≤ λ ≤ 800 nm), the plasma frequency and corresponding dielectric constant become negative, which leads the refractive index to imaginary[22]. A shrunk imaginary part of the refractive index, in turn, slumped absorption and boomed transmission[46], which is also noted from the skin depth spectra. Moreover, refractive index can provide information about the microstructure of thin films since it is responsive to structural defects (such as voids, dopants, inclusions). A similar result was obtained by Abed et al.[47].

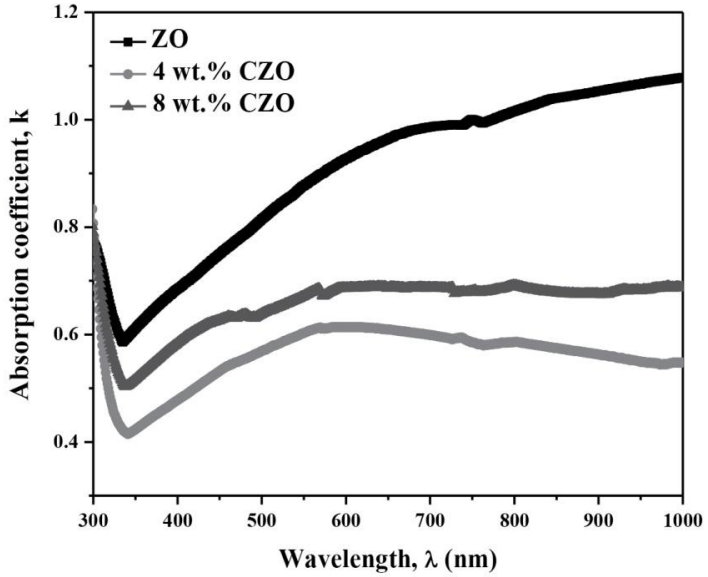

Fig. 7. Absorption coefficient vs wavelength spectra for ZO and CZO thin films.

Variation of k with respect to the incident electromagnetic radiation, λ of ZO and CZO, has been shown in **Fig. 7.** The values of k calculated by using the following equation (8):

$$k = \frac{\alpha\lambda}{4\pi} \tag{8}$$

It is clear from the above equation that k depends on the absorption coefficient α and the λ of the incident photon. The curve exhibits a lowering trend with the increase of wavelength, and after experiencing a transition at around 337 nm, all the samples went upward and then became linear at higher wavelengths around 600 nm. This kind of trend was also observed by **Abeda et al**[47].

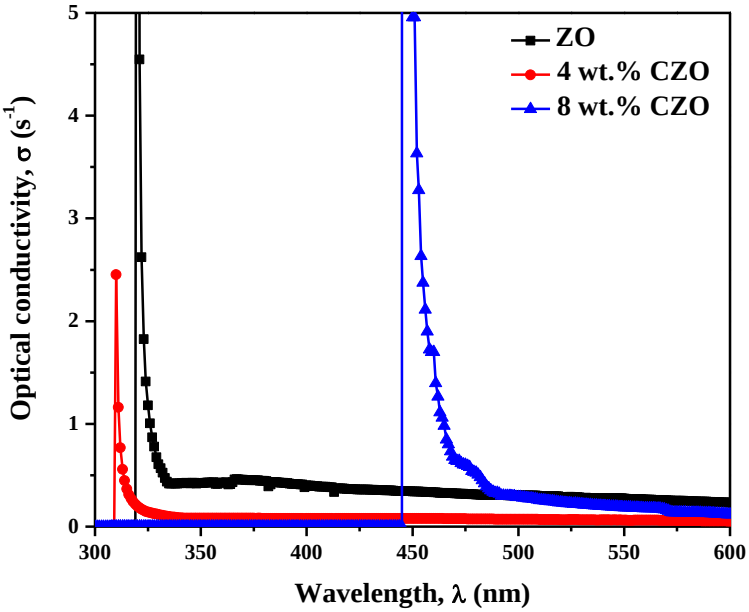

Fig. 8. Optical Conductivity vs wavelength spectra for ZO and CZO thin films.

Fig. 8 shows that optical conductivity has a maximum value in the UV region for all the samples. As the frequency ascent, optical conductivity declined progressively. While in the visible region, 8 wt.% CZO exhibits higher optical conductivity among all the samples. High optical conductivity indicates their high photo-response nature, which suggests that a particular composition is compatible for optoelectronic device application[48].

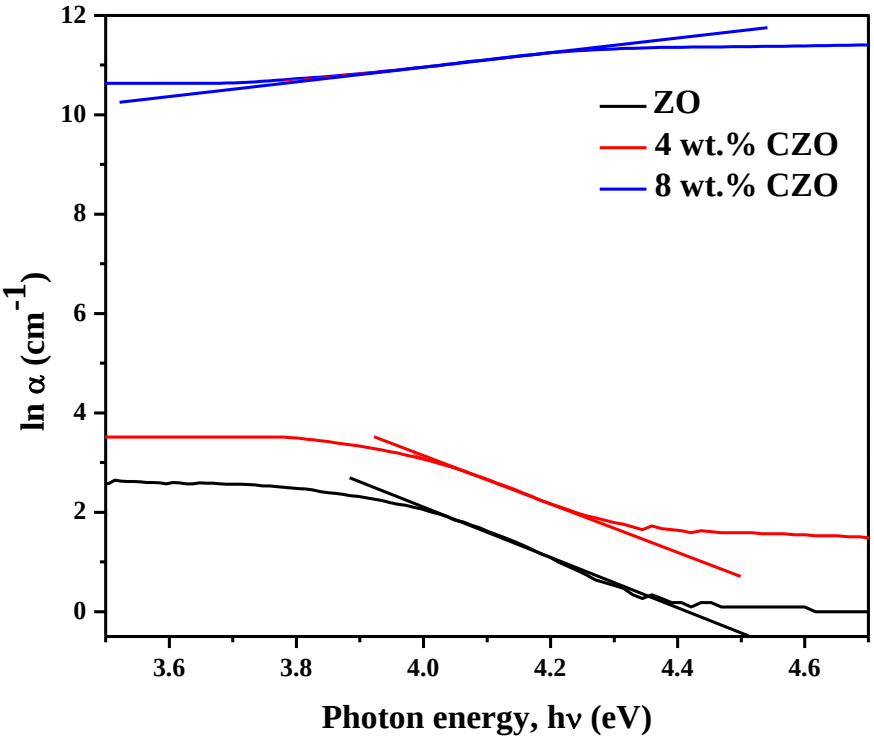

Fig. 9. Urbach energy spectra for ZO and CZO thin films.

Urbach energy refers to a parameter used to describe the exponential tail in the absorption spectra of a material. It quantifies the extent of disorder or imperfections in the structure of the material and provides insights into the localized electronic states near the band edges[48].

The ln(α) vs hν near the absorption edge is shown in **Fig. 9** The reciprocal of the slope of the obtained straight lines leads to determining the Urbach energy E_u. The obtained band tail width values are tabulated in Table 1. The value of E_u is increased from 0.19 eV to 0.75 eV with the increase in Cu doping percentage. This behavior is attributed to the Cu content in the ZO matrix, which drives the rise to atomic disorder and defects in the structural bond. The disorder and defects can induce localized states at or near the conduction band, which leads increase in the band tail width E_U[49,50]. Urbach energy refers to the quality of thin films[51].

Electrical Analysis

Resistivity (ρ) is a measure of the inherent resistance of a material to the flow of electric current. It quantifies the resistance experienced by a unit volume of material when a unit potential difference is applied across its ends. Resistivity is typically represented by the Greek letter ρ and has the unit of ohm-meter (Ω·m).

Sheet resistance (R_s) is a closely related parameter that specifically refers to the resistance per square of a thin film. It is a two-dimensional measure of electrical resistance and is commonly used to characterize the conductivity of thin films. Sheet resistance is determined by dividing the resistivity of the material by its thickness and is expressed in units of ohms per square (Ω/sq).

In the context of Cu-doped zinc oxide (CZO) thin films, the resistivity and sheet resistance can be influenced by the concentration of Cu dopants. The corresponding values of ρ and R_s are cited in **Table 2**.

Increasing Cu doping concentration in ZO thin films leads to a decrease in resistivity and sheet resistance. This behavior can be attributed to several factors. Firstly, the introduction of Cu dopants can enhance the carrier concentration in the ZO thin film. Cu dopants can donate additional electrons to the ZO lattice, increasing the overall carrier density and improving the conductivity of the material[52]. The increased carrier concentration reduces the resistance encountered by the electric current, resulting in lower resistivity and sheet resistance values[53]. Similar results ascribed by Omri et al., Singh et al., and others [53, 54, 55, 56,57,58]. Joshi et al.[59] recorded a drastic decrease in the value of resistivity from about 1600 Ω-cm to 172 Ω-cm for 3% CZO and from 172 Ω-cm to 82 Ω-cm for 6% CZO.

Compared to this value, our samples showed high resistance of about 2272 Ω-cm for ZO, and with the increase of Cu wt.%, the decrease in resistivity is moderate of about 1169 Ω-cm for 4% CZO and 940 Ω-cm for 8 wt.% CZO. Licurgo et al.[60] also showed a decrease in resistivity with the increase in Cu concentration. The resistivity value changes from 6.58 Ω-cm to 2.93 Ω-cm for ZO to 7.5 wt.% CZO, respectively. Literatures mostly describe increasing carrier concentration as the reason for decreasing resistivity.

Secondly, Cu dopants can also improve the mobility of charge carriers in the ZO thin film[52]. This means that the charge carriers can move more freely through the lattice, experiencing fewer scattering events and encountering less resistance[60]. As a result, the resistivity and sheet resistance decrease. This enhanced conductivity can be beneficial for various applications, such as in transparent conductive coatings for optoelectronic devices, where low resistivity and high conductivity are desired.

Furthermore, Cu dopants can also alter the defect structure and microstructure of the ZO thin film. This can lead to the reduction of grain boundaries, defects, and other scattering centers, which impede the movement of charge carriers. The decrease in these scattering sources further contributes to the reduction in resistivity and sheet resistance.

Overall, our results demonstrate that copper doping in ZO thin films significantly influences their optical and electrical properties. The redshift in the absorption edge and the increase in bandgap energy indicate the modification of the ZO electronic structure due to copper incorporation. These findings provide valuable insights for the design and optimization of CZO thin films for various optoelectronic applications.

Table-2. The values of optical conductivity, resistivity, and sheet resistance

Composition	Optical Conductivity, σ_{opt} (S^{-1}) at 500 nm	Resistivity, $\rho \times 10^3$ (Ω-cm)	Sheet Resistance, $R_S \times 10^7$ (Ω-sq)
ZO	10.359	2.272	4.6083
4% CZO	4.65402	1.161	3.43644
8% CZO	33.6725	0.940	2.31962

IV. Conclusion

This work has investigated the optical properties of thin films and provided valuable insights into their behavior and potential applications. By investigating the optical response of the thin films, we have expanded a deeper understanding of their properties and explored the factors influencing their optical behavior. Our analysis demonstrated that Cu doping into ZO significantly increases the transmittance of the deposited films. The transmittance went to 90% for 8 wt.% CZO. The optical bandgap energy and Urbach energy are augmented with the increase of Cu dopant wt. percentage. Moreover, the optical conductivity and resistivity curves have synchronized. In conclusion, there is great promise for a variety of applications with the synthesis of CZO (Cu-doped ZnO) thin films by an easy, efficient, and cost-effective technique. One noteworthy use is in gas sensing, where the enhanced conductivity and specific characteristics of CZO thin films enable the detection and analysis of various gases. Gas sensor devices can benefit from CZO thin films because of their enhanced carrier concentration, which can be achieved through Cu doping and leads to more effective charge transport. Strongly Cu-doped ZO thin films show quantum confinement effects in their optical characteristics, providing new opportunities for band gap engineering. Within the ZO thin film, nanocrystalline areas can be generated by varying the concentration of Cu doping. The quantum confinement effects are introduced by these nanocrystalline areas.

Acknowledgement

The authors wish to acknowledge Muhammad R. Islam and department of Physics, Bangladesh University of Engineering and Technology, Dhaka-1000, Bangladesh for their support and for providing necessary laboratory facilities in completing this experiment.

Conflict of Interest

The author(s) have no conflicts to disclose.

Author Contributions

Muhammad G. Azam carried out the experiment and fabricated the samples. **Kazi Zahanara Islam** wrote the manuscript with support from **Muhammad G. Azam and Md. Borhanul Asfia.** Mutually author(s) discussed the result and contributed to the final manuscript.

Data availability statement

The data that support the findings of this study are available from the corresponding author Kazi Zahanara Islam, islam.zahanara@gmail.com and Muhammad G. Azam, azamm0081@gmail.com, Md. Borhanul Asfia, upon reasonable request.

References

1. Khan Z.R., M.S. Khan, M. Zulfequar, M.S. Khan, Optical and Structural Properties of ZnO Thin Films Fabricated by Sol-Gel Method, Mater. Sci. Appl. 2 (2) 340 (2011). 10.4236/msa.2011.25044

2. Janotti C.G. A., Van de Walle, Aluminum Doped ZnO Thin Films Using Chemical Spray Pyrolysis, Rep. Prog. Phys. 72, (1–29) 126501 (2009). http://dx.doi.org/10.1088/0034-4885/72/12/126501

3. Sharmin M., A.H. Bhuiyan, Modifications in structure, surface morphology, optical and electrical properties of ZnO thin films with low boron doping, J. Mater. Sci. Mater. (2019). https://doi.org/10.1007/s10854-019-00781-8

4. Özgür Ü., Ya.I. Alivov, C. Liu, A. Teke, M.A. Reshchikov, S. Doğan, V. Avrutin, S.-J. Cho, and H. Morkoçd, A comprehensive review of ZnO materials and devices, J. Appl. Phys. 98(4) 041301 (2005). https://doi.org/10.1063/1.1992666

5. Kazeminezhad I., S. Saadatmand, R. Yousefi, Bull., Effect of transition metal elements on the structural and optical properties of ZnO nanoparticles, Mater. Sci. (2015). https://doi.org/10.1007/s12034-016-1206-y

6. Pearton S.J., D.P. Norton, M.P. Ivill, A.F. Hebard, J.M. Zavada, W.M. Chen, I.A. Buyanova, Nanoparticles of Ni in ZnO single crystal matrix, IEEE T. Electron. Dev. 54(5) 1040 (2007). https://doi.org/10.1140/epjb/e2013-40008-5

7. Kim K. -T., G. -H. Kim, J. -C. Woo, C. -I. Kim, Characteristics of Nickel-doped Zinc Oxide thin films prepared by sol–gel method, Surf. Coat. Technol. 202 (22-23) 5650 (2008). https://doi.org/10.1016/j.surfcoat.2008.06.078

8. Voicu G., D. Miu, C.-D. Ghitulica, S.-I. Jinga, A.-I. Nicoara, C. Busuioc, A.-M. Holban, Co doped ZnO thin films deposited by spin coating as antibacterial coating for metallic implants, Ceram. Int. (2019). https://doi.org/10.1016/j.ceramint.2019.10.118

9. Hu D., X. Liu, S. Deng, Y. Liu, Z. Feng, B. Han, Y. Wang, Y. Wang, Structural and optical properties of Mn-doped ZnO nanocrystalline thin films with the different dopant concentrations, Physica E Low Dimens. Syst. Nanostruct. 61, 14-22 (2014). https://doi.org/10.1016/j.physe.2014.03.007

10. Agarwal D.C., U.B. Singh, S. Gupta, R. Singhal, P.K. Kulriya, F. Singh, A. Tripathi, J. Singh, U. S. Joshi, D. K. Avasthi, Enhanced room temperature ferromagnetism and green photoluminescence in Cu doped ZnO thin film synthesised by neutral beam sputtering, Sci. Rep. 9, 6675 (2019). https://doi.org/10.1038/s41598-019-43184-9

11. Islam M.R., M.G. Azam, Enhanced photocatalytic activity of Mg-doped ZnO thin films prepared by sol–gel method, Surf. Eng., 37(6), 775-783, 2021. https://doi.org/10.1080/02670844.2020.1801143

12. Sonia S., I.J. Annsi, P.S. Kumar, D. Mangalaraj, C. Viswanathan, N. Ponpandian, Hydrothermal synthesis of novel Zn doped CuO nanoflowers as an efficient photodegradation material for textile dyes, Mater. Lett. 144, 127 (2015). 10.1016/j.matlet.2015.01.026

13. Karthik K.V., A.V. Raghu, K.R. Reddy, R. Ravishankar, M. Sangeeta, N.P. Shetti, C.V. Reddy, Green synthesis of Cu-doped ZnO nanoparticles and its application for the photocatalytic degradation of hazardous organic pollutants, Chemosphere 287, 132081 (2022). https://doi.org/10.1016/j.chemosphere.2021.132081

14. Khalid A., P. AhmadI, A.I. Alharthi, S. Muhammad, M.U. Khandaker, M.R.I. Faruque, I.U. Din, M. A. Alotaibi, A. Khan, Synergistic effects of Cu-doped ZnO nanoantibiotic against Gram-positive bacterial strains, PLoS One 16(5), (2021). https://doi.org/10.1371/journal.pone.0251082

15. Urbach F., The Long-Wavelength Edge of Photographic Sensitivity and of the Electronic Absorption of Solids, Phys. Rev. 92, 1324 (1953). https://doi.org/10.1103/PhysRev.92.1324

16. EI-Hagary M., M.E. Ismail, E.R. Shaaban, A. EI-Taher, Effect of γ-irradiation exposure on optical properties of chalcogenide glasses Se70S30−xSbx thin films, Rad. Phys. Chem. 81, 1572 (2012). https://doi.org/10.1016/j.radphyschem.2012.05.012

17. Omer M.A., Elementary Solid State Physics, Addison-Wesley Publishing (1975).

18. Agashe A., S. S. Major, Electron Scattering Mechanism of FTO Films Grown by Spray Pyrolysis Method, J. Mater. Sci. 31, 2965 (1996). https://doi.org/10.1007/s11664-010-1225-1

19. Moholkar A.V., S.M. Pawar, K.Y. Rajpure, P.S. Patil, C.H. Bhosale, Properties of highly oriented spray-deposited fluorine-doped tin oxide thin films on glass substrates of different thickness, J. Phys. Chem. Solids 68 (10), 1981-1988 (2007). https://doi.org/10.1016/j.jpcs.2007.06.024

20. Hassanien , A.A. Akl, Effect of Se addition on optical and electrical properties of chalcogenide CdSSe thin films, Superlattices Microstruct. 89, 153-169 (2016). https://doi.org/10.1016/j.spmi.2015.10.044

21. Joshi K., M. Rawat, S.K. Gautam, R.G. Singh, R.C. Ramola, F. Singh, Band gap widening and narrowing in Cu-doped ZnO thin films, J. Alloys Compd. 680, 252-258 (2016). https://doi.org/10.1016/j.jallcom.2016.04.093

22. Hassanien A.S., A.A. Akl, Influence of composition on optical and dispersion parameters of thermally evaporated non-crystalline Cd50S50−xSex thin films, J. Alloys Compd. 648, 280-290 (2015). https://doi.org/10.1016/j.jallcom.2015.06.231

23. Van Zeghbroec B., Principle of Electronic Devices: Principle of Semiconductor Devices, (1997).

24. Tauc J., in: J. Tauc (Ed.), Amorphous and Liquid Semiconductors, Plenum Press, London and New York, (1974).

25. Davis E.A., N.F. Mott, Conduction in non-crystalline systems V. Conductivity, optical absorption and photoconductivity in amorphous semiconductors, Philos. Mag. 22 (179), 0903-0922 (1970). 10.1080/14786437008221061

26. Alireza S., A. F. Ismail, N. Hadi, Z. Othaman, M. K. Mustafa, Spectral features and antibacterial properties of Cu-doped ZnO nanoparticles prepared by sol-gel method Chin. Phys. B 25(7), 077803, (2016). https://cpb.iphy.ac.cn/article/2016/1836/cpb_25_7_077803.html